

Soil Capillary Fringe Depression Caused by LNAPL Contamination in a Variational Hydraulic Gradient

Harris Ramli¹, Kapil Kumar¹, Tan Zhi Hern¹ and Mastura Azmi¹

Abstract - A two-dimensional experiments were carried out to assess the capillary depression in the soil and the migration radius of the contaminant plume prior to lateral migration caused by a diesel spill, while considering various hydraulic gradients ranging from 0.714 to 3.571. A Simplified Image Analysis Method (SIAM) was utilised due to the dynamic nature of the experiment. Based on the study, deeper diesel migration occurs in larger spilled volumes because the pressure is high enough to overcome capillary forces, and it eventually depresses the capillary fringe layer. When comparing hydraulic gradients with high and low values, it can be observed that the low hydraulic gradient results in more capillary depression. As a result, pollutants would be significantly closer to the groundwater layer. The radius of the vertical contamination plume prior to the lateral migration reveals that even with a high hydraulic gradient, the maximum contamination plume size prior to the lateral migration is the same as any other hydraulic gradient. However, in the high hydraulic gradient, LNAPL migration accelerates with increasing hydraulic gradient, leading to soil and groundwater contamination at discharge points and throughout the entire groundwater pathway.

Keywords – LNAPL Contamination, Groundwater Hydraulic Gradient, Capillary Fringe Depression, Contamination Plume, Lateral Migration.

I. INTRODUCTION

Non-aqueous phase liquids (NAPLs) are any liquids or organic compounds that do not dissolve or are immiscible in water. Products refined from crude oil are one of the most common examples of NAPLs that do not dissolve or mix well with water. NAPLs are classified into two types based on their density relative to water, light non-aqueous phase liquids (LNAPL) and dense non-aqueous phase liquids (DNAPL). In simple terms, LNAPL is lighter than water, whereas DNAPL is heavier while water consider having a density of 1.0 g/cm³. LNAPL density is typically between 0.6 and 0.9 g/cm³, whereas DNAPL density can reach up to 1.7 g/cm³. The density of NAPLs can vary depending on the chemical compound and composition of the LNAPL or DNAPL. Due to the low density of LNAPL, oil or LNAPL product spills always pose a significant hazard because the pollutant flows farther from the release point. This condition complicates the cleaning and soil remediation processes and also poses a risk of groundwater contamination. The contamination will not only affect groundwater and soil, but it will also produce Green House Gases that will last for several decades [1].

LNAPL products can be composed of pure organic compounds or, like diesel and gasoline, a complex mixture of numerous compounds. The various LNAPL components may dissolve in the aqueous phase in small concentrations, according to their respective water solubilities. Unfortunately, even at extremely low concentrations of a few parts per billion (ppb), some chemical compounds in drinking water can be harmful to humans. Furthermore, the immiscible properties of LNAPL cause a slow dissolution process, resulting in long-term contamination.

Every year, millions of barrels of oil are extracted from the earth's surface, and due to the immense quantity of oil that must be managed, the oil industry faces the risk of accidental discharges into the ground and surface water as a result of tanker accidents, pipeline ruptures, or storage tank failures. With this condition, if the contamination discharge occurs underground, it won't be detected until a nearby drinking water well becomes contaminated. In some cases, only due to large-scale accidents, groundwater contamination by other LNAPL is discovered as a result of the required soil investigation [2]. Groundwater contamination by LNAPL, such as diesel, is known to increase environmental and health risks due to their toxicity and carcinogenic compounds such as benzene, toluene, ethylbenzene and xylene (BTEX).

Since the 1970s, when the impact of LNAPL spills on groundwater became a global concern, soil remediation techniques have been improved. Even though the technique has evolved alongside new technologies over the past half century, remediation performance is still difficult to attain in a short period of time. An industrial-scale spill accident would require more than ten years to clean up, and there have been instances in which diesel contamination has contaminated municipal wells, despite the fact that the contamination source is not in the direction of groundwater flow [3].

The inability to fully understand the LNAPL migration behaviour is one of the leading causes of the problem's complexity and the difficulty of achieving the required residual LNAPL saturation target in remediation projects. Thus, the main aim of this research is to investigate the capillary depression in the soil and the migration radius of the contaminant plume prior to the occurrence of lateral migration caused by a diesel spill, while considering various hydraulic gradients. This research will provide an insight of the lateral migration behaviour of LNAPL in natural environments with groundwater flow. A Simplified Image Analysis Method (SIAM) was employed to ensure that all necessary data was captured, given that the experiment will be conducted under dynamic conditions involving diesel migration and groundwater flow in the subsurface

¹School of Civil Engineering, Engineering Campus, Universiti Sains Malaysia, 14300, Nibong Tebal, Penang, Malaysia

II. SIMPLIFIED IMAGE ANALYSIS METHOD (SIAM) AND EXPERIMENTAL WORK

The SIAM is a method capable of instantaneously measuring the saturation distribution values for water and NAPL in granular soils for the whole range of large domains [4]. This method is regarded as a non-destructive and non-intrusive method for determining the spatial and temporal distribution of fluid saturations throughout the entire domain. In order to derive the saturation distribution matrices for water ($[S_w]$) and LNAPL ($[S_o]$), the average optical densities of each matrix element (D_i) are compared with the average optical densities of the domain fully saturated with water (D_i^w), LNAPL (D_i^o), and completely dry (D_i^d), using the Beer-Lambert Law of Transmissivity.

Two consumer-grade digital cameras, each equipped with a two distinct band-pass filter (i and j), were utilised to acquire the optical density data. The average optical density (D_i) is calculated for the intensity of reflected light in a digital image according to Equation (1), where N represents the number of pixels in the area of interest and, for a specific spectral band i , d_{ji} denotes the optical density of individual pixels, I_{ji}^r signifies the intensity of the reflected light as determined by the values of individual pixels, and I_{ji}^o signifies the intensity of light that is reflected by an ideal white surface [5]. To calculate the average optical density values for every mesh element in the studied domain, one can utilise Equation (2) to generate a matrix of correlations

$$D_i = \frac{1}{N} \sum_{j=1}^N d_{ji} = \frac{1}{N} \sum_{j=1}^N \left[-\log_{10} \left(\frac{I_{ji}^r}{I_{ji}^o} \right) \right] \tag{1}$$

$$\begin{bmatrix} D_i \\ D_j \end{bmatrix}_{mn} = \begin{bmatrix} (D_i^w - D_i^d)S_w + (D_i^o - D_i^d)S_o + D_i^d \\ (D_j^w - D_j^d)S_w + (D_j^o - D_j^d)S_o + D_j^d \end{bmatrix}_{mn} \tag{2}$$

Three calibrating photographs are necessary for the calibration process (D_i^w , D_i^o , and D_i^d). These photographs correspond to the boundaries of the relationship plane and include the following: dry sand ($S_w = 0\%$, $S_o = 0\%$), sand completely saturated with LNAPL ($S_w = 0\%$, $S_o = 100\%$), and sand completely saturated with water ($S_w = 100\%$, $S_o = 0\%$). The values of $[S_w]$ and $[S_o]$ represent water saturation and NAPL saturation, respectively, as illustrated in Fig. 1.

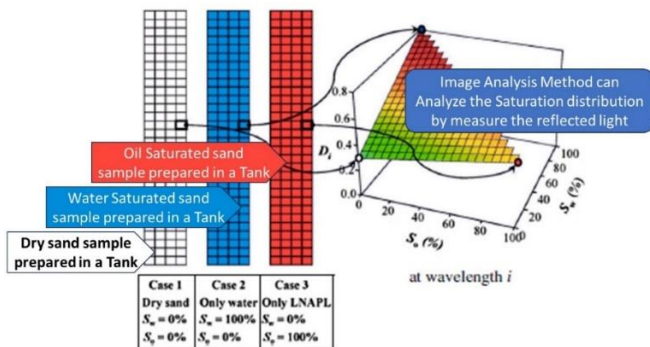


Fig. 1 Concept of Simplified Image Analysis Method (modified after [6])

In order to improve the visibility of diesel and increase the light absorption capacity of water, Brilliant Blue FCF dye was utilised for water and Red Sudan III dye was employed for diesel. Both dyes were used at concentrations of 1:10,000 by weight, without any noticeable change in the physical properties of water and diesel. The soil particles neither absorb nor filter the dyes.

The study of diesel's two-dimensional lateral migration in porous media (sand) was conducted using a tank (size: 700 mm x 550 mm x 35 mm) equipped with transparent acrylic walls. The tank was configured as showed in the Fig. 2. Utilizing LED floodlights as a controlled lighting source, the experiment was conducted in a darkened room. For image capture, DSLR cameras equipped with 450 and 656 nm band-pass filters were set up. Throughout the experiment, photographs were captured at 15-minute intervals.

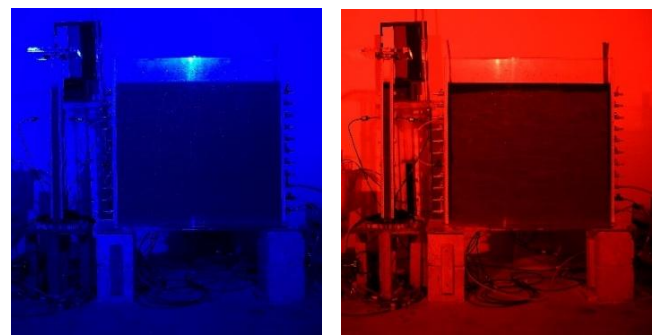


Fig. 2 Tank setup before experiment start (fully saturated with water)

Using Nikon ViewNX 2.10.3, every image was converted from NEF (Nikon proprietary RAW version files) to TIFF (Tagged Image File Format). The TIFF images underwent analysis using a MATLAB R2022b programme that was developed internally. Both photos were analysed in MATLAB R2022b with 450 nm and 656 nm band-pass filters, and the saturation of diesel and water was transferred to an Excel workbook for analysis.

To assess diesel migration in relation to groundwater flow, water circulation was established to simulate the groundwater table and ensure groundwater flow in a unidirectional direction. In order to replicate varying degrees of contamination severity, distinct hydraulic gradients (0.714, 2.413, 3.571) were established, and 125ml and 250ml volumes of diesel were introduced (Table 1).

TABLE I Volume of oil spill and hydraulic gradient for each experiment

Experiment	Oil Spill Volume (ml)	Hydraulic Gradient, i
H 3.5	250	3.571
L 3.5	125	3.571
H 2.4	250	2.413
L 2.4	125	2.413
H 0.7	250	0.714
L 0.7	125	0.714

III. CAPILLARY FRINGE DEPRESSION AND CONTAMINATION PLUME

At the start of the experiment, the fully saturated sand was allowed to drain by gravitational force. Stable capillary fringe height could be observed in less than six hours, as a result of the water draining relatively rapidly due to the high permeability of sand. The diesel migrated downward as a result of gravitational force and capillarity after it spilled from the top of the tank. When a diesel spill volume of 250 mL is compared to 125 mL, the former rapidly migrate to the capillary fringe layer.

The diesel distribution result at the end of the experiment for experiments H 2.4 and L 2.4 is presented in Fig. 3 and Fig. 4, respectively. It was observed that a greater quantity of diesel had already infiltrated the capillary fringe area in the 250 mL diesel spill (H 2.4) than in the 125 mL diesel spill (L 2.4).

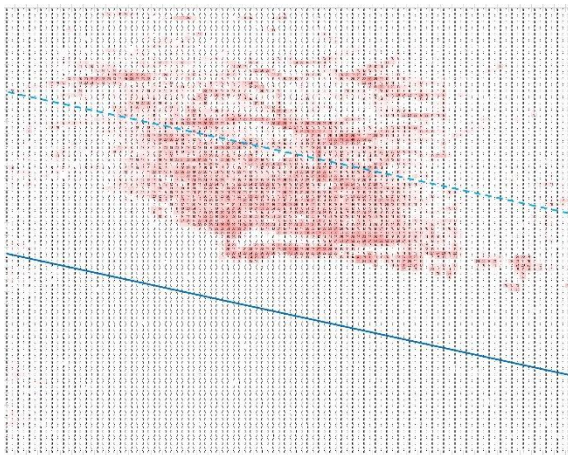


Fig. 3 Distribution of diesel in the tank at the end of Experiment H 2.4.

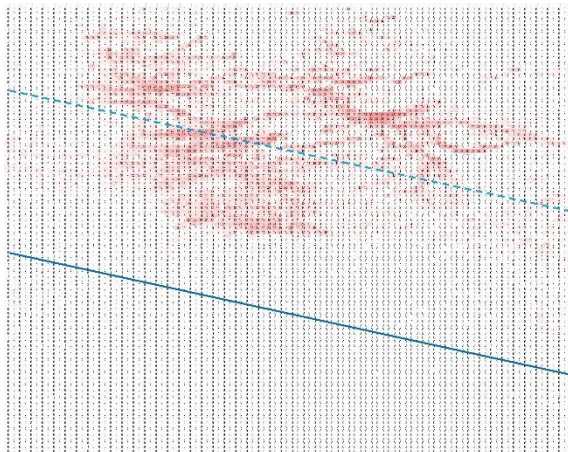


Fig. 4 Distribution of diesel in the tank at the end of Experiment L 2.4.

In the case of larger diesel spills, a greater quantity of diesel would reach the capillary fringe layer. As a result, pollutants would be significantly closer to the groundwater layer. Under natural groundwater fluctuations, the layer contaminated with diesel would come into contact with the rising groundwater level. Primarily, this will contribute to the contamination of the

groundwater. An area with high annual rainfall would have more frequent fluctuations in groundwater levels, which would expose natural groundwater to contaminated layers more frequently.

Additionally, deeper diesel migration occurs in a larger spilled volume because it has sufficient pressure to overcome the capillary forces in order to advance into the finer pores filled with water. The risk of groundwater contamination would increase if there was a larger leak of LNAPL at the location. With respect to the experiment that was conducted, diesel would likely reach the groundwater level if the volume of diesel spilled were to double that of the current release.

When comparing LNAPL to DNAPL, if DNAPL is the source of contamination, the contamination would likely move to the greatest depth possible given the volume of the available spill. Despite the potential for the DNAPL migration to extend to deeper soil layers, the pollution continues to persist in the local vicinity of the origin. On the contrary, LNAPL, being less dense than water, it will float on the surface of the groundwater and continue to flow down the groundwater pathway until its whole mobilised volume is depleted.

In both spills (240 mL and 125 mL), the diesel is only able to infiltrate up until the capillary fringe layer and depress the original height of capillary fringe. The capillary fringe is a subsurface layer situated between the saturated and unsaturated zones. Groundwater seeps up through capillary action to fill pores in this layer. LNAPL spilling usually moves downward, causing the capillary fringe to become depressed. This study investigated the changes in the capillary fringe at the point of contamination release.

Fig. 5 shows a graph of the maximum depression from each test against the corresponding hydraulic gradients. A relationship can also be observed between hydraulic gradient and capillary fringe depression. When comparing hydraulic gradients with high and low values, it can be observed that the low hydraulic gradient results in more capillary depression. Diesel migrates laterally at a faster pace when the hydraulic gradient increases, due to the hydraulic gradient's incline and the reduced depression of the capillary fringe. The similar trend in the volumes of both oil spills supports this relationship

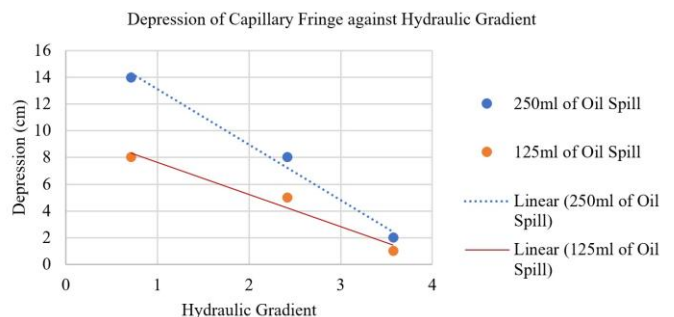


Fig. 5 Capillaries fringe depression against hydraulic gradient

Comparing various intensities of diesel spills reveals that as the amount of the diesel spill increases, so does the depression of the capillary fringe. This is due to the fact that as the amount of the diesel spill increases, so does the weight of LNAPL, which provides it with greater energy to depress the capillary

fringe. Returning to the mechanics of contamination migration that have already been discussed, the capillary fringe serves as a crucial barrier to the saturated layer; as this barrier thins, more contaminants will come into direct contact with the groundwater, raising the possibility of groundwater contamination.

In relation to Fig. 5, because of the greater capillary depressions in the case of experiment H 0.7, where the hydraulic gradient is low and the diesel spill is high, diesel will be much closer to the saturation zone. The degree of contamination at the exact spill source would be greater in comparison to any other experiment.

The degree of contamination at the exact spill source in experiments with a high hydraulic gradient is likely to be less than in experiments with a low hydraulic gradient, but it will flow much further from the source. This is because the mobilised diesel would be more easily migrated laterally as opposed to vertically, under conditions of high hydraulic gradients. Diesel will continue to flow down the groundwater pathway until its entire mobilised volume is depleted, as it floats on the surface due to its lower density in comparison to water.

As the groundwater is discharged to the surface water body in the freshwater storage as part of the natural water cycle, subsequent processes including evaporation, condensation, and precipitation serve to replenish the groundwater. When the volume of the diesel spill was sufficient to flow to a greater extent of the groundwater path, as the natural water cycle progressed, it would likely reach surface water. Consequently, under conditions of high hydraulic gradient, contamination of the soil and groundwater not only occurs at the point of discharge but also extends along the entire pathway to reach the surface water or even the drinking water supply well.

In this study, the maximum radius of the vertical contamination plume was also analysed based on the data obtained in every photo taken. This is the size of the contamination plume prior to its lateral migration caused by the hydraulic gradient. This analysis can provide a more precise depiction of the lateral spread of diesel on-site as a result of the migration patterns of LNAPL to the left and right of the point of contamination.

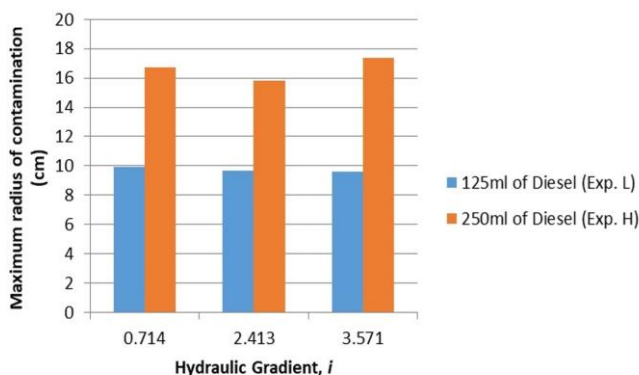


Fig. 6 Maximum radius of the vertical contamination plume

As shown in Fig. 6, a bar chart reveals the maximum radius of the vertical contamination plume for various volumes of oil spill and hydraulic gradient. As indicated by the bar graph, the radius of the vertical contamination plume will be influenced by the severity of the diesel spill volume. Due to the fact that this condition occurs in an unsaturated zone, the air present in the soil void will be replaced by the available LNAPL. The ability of LNAPL to migrate and flow is directly correlated with its volume, as a greater quantity of LNAPL increases the pressure to fill voids in soil pores with the available mobilised LNAPL. Hence, as the volume of the LNAPL spill increases, so does the radius of the contamination plume prior to its lateral migration.

This analysis also reveals that even with a high hydraulic gradient, the maximum contamination plume size prior to lateral migration is the same as any other hydraulic gradient. This is because the hydraulic gradient would only be effective when the contamination started to migrate laterally.

IV. CONCLUSION

This study is conducted to investigate the capillary depression in the soil and the migration radius of the contaminant plume prior to the occurrence of lateral migration caused by a diesel spill, while considering various hydraulic gradients ranging from 0.714 to 3.571. Due to the dynamic nature of the experiment, which included diesel migration and subsurface groundwater flow, a Simplified Image Analysis Method (SIAM) was utilised. Based on the study, deeper diesel migration occurs in larger spilled volumes because the pressure is high enough to overcome capillary forces, and it eventually depresses the capillary fringe layer. As a result, pollutants would be significantly closer to the groundwater layer. When comparing hydraulic gradients with high and low values, it can be observed that the low hydraulic gradient results in more capillary depression. Diesel migrates laterally at a faster pace when the hydraulic gradient increases, due to the hydraulic gradient's incline and the reduced depression of the capillary fringe. Consequently, under conditions of high hydraulic gradient, contamination of the soil and groundwater not only occurs at the point of discharge but also extends along the entire groundwater pathway. In the analysis of the radius of the vertical contamination plume prior to the lateral migration, it will be influenced by the severity of the diesel spill volume. This analysis also reveals that even with a high hydraulic gradient, the maximum contamination plume size prior to lateral migration is the same as any other hydraulic gradient.

V. ACKNOWLEDGEMENT

The authors wish to express sincere appreciation for the support from Universiti Sains Malaysia in making this project a success. The research was funded by the Ministry of Higher Education Malaysia under the LRGS-MRUN 2016-1 Grant Scheme with grant number LRGS/1/2016/UTM/01/1/3.

REFERENCES

- [1] Sookhak Lari, K., Davis, G. B., Bastow, T., & Rayner, J. L. (2024). On quantifying global carbon emission from oil contaminated lands over

- centuries. *Science of the Total Environment*. 907. Available: <https://doi.org/10.1016/j.scitotenv.2023.168039>
- [2] Liu, Y., Zhao, X., Wang, X., Ding, A., & Zhang, D. (2024). Application of whole-cell bioreporters for ecological risk assessment and bioremediation potential evaluation after a benzene exceedance accident in groundwater in Lanzhou, China. *Science of the Total Environment*. 906. Available: <https://doi.org/10.1016/j.scitotenv.2023.168039>
- [3] Ahad, J. M. E., Martel, R., & Calderhead, A. I. (2023). Isotope forensics of polycyclic aromatic compounds (PACs) in a contaminated shallow aquifer. *Chemosphere*. 140169. Available: <https://doi.org/10.1016/j.chemosphere.2023.140169>
- [4] Flores, G., Katsumi, T., Inui, T., & Kamon, M. (2011). A Simplified Image Analysis Method to Study LNAPL Migration in Porous Media. *Soils and Foundations*, 51(5), pp. 835–847.
- [5] Kechavarzi, C., Soga, K., & Wiart, P. (2000). Multispectral image analysis method to determine dynamic fluid saturation distribution in two-dimensional three-fluid phase flow laboratory experiments. *Journal of Contaminant Hydrology*, 46(3–4), pp. 265–293.
- [6] Yimsiri, S., Euaapiwatch, S., Flores, G., Katsumi, T., & Likitlersuang, S. (2018). Effects of water table fluctuation on diesel fuel migration in one-dimensional laboratory study. *European Journal of Environmental and Civil Engineering*, 22(3), pp. 359–385.